# Computation of Reacting Flowfield with Radiation Interaction in Chemical Lasers

Victor Quan,* Saul F. Persselin,† and Tien Tsai Yang‡
*Rockwell International/Rocketdyne Division, Canoga Park, California*

**A numerical procedure has been developed to provide a rapid and stable solution of the reacting and radiating flowfield in chemical laser cavities. A marching technique, implicit in both fluid mechanics and chemistry, is employed in solving the two-dimensional mixing layer equations. The aerokinetics and radiation interaction is calculated iteratively by solving the aerokinetic equations for the gain distribution and the propagation equations for the radiation field. In the iterative solution, a linearization method which leads to enhanced numerical efficiency is employed.**

## Nomenclature

$C_p$ = specific heat at constant pressure
$D$ = mass diffusion coefficient
$F$ = species mole-mass ratio
$h$ = enthalpy
$I$ = radiation intensity
$k$ = thermal conductivity
$k_f, k_b$ = forward and backward reaction rate constants
$p$ = pressure
$s$ = species production rate due to chemical reactions and radiative transitions
$T$ = temperature
$u$ = axial velocity
$v$ = lateral velocity
$\dot{w}$ = species production rate due to chemical reactions
$x$ = axial distance
$y$ = lateral distance
$y_m$ = nozzle pair centerline-to-centerline distance
$\alpha$ = gain
$\epsilon$ = photon energy; $\epsilon = 1$ for radial flow and 0 for linear flow
$\eta$ = normalized lateral distance, $y/y_m$
$\mu$ = viscosity
$\nu$ = stoichiometric coefficient
$\rho$ = density
$\sigma$ = 1 for axisymmetric flow and 0 for planar flow

*Subscripts*

$b$ = basic solution
$i,j$ = species
$J$ = rotational transition state
$K$ = axial grid point
$v$ = vibrational transition level

*Superscript*

$L$ = lateral grid point

## Introduction

In a chemical laser, the gaseous reactants are injected into the laser cavity. The subsequent mixing and chemical reactions produce excited species which undergo radiation transitions. The emitted radiation, upon striking the mirrors, are partially reflected into the reacting flow medium. Modeling and solution of the chemical laser system, thus, require the simultaneous consideration of the convective and mixing processes, chemical reactions, and radiative transports.

There exist various numerical treatments of chemical laser performance, e.g., Refs. 1-5. Due to the complex aerokinetics-radiation interaction, however, these analyses generally employ either simplified optical or fluid mechanical models in order to avoid prohibitively long computation time. For example, LAMP or ALFA,[1,2] which is a widely used computer program in the chemical laser industry,[6-8] treats fluid mechanics in detail; but it allows for only plane parallel mirrors (Fabry-Perot cavity). On the other hand, in studies involving general optics, such as a rooftop resonator,[5] a quasi-one-dimensional fluid mechanics approach (scheduled mixing) commonly is used.

The objective of the present work is to formulate a numerical procedure and develop a computer program to provide a rapid and accurate solution for the coupled aerokinetics-optics interaction problem involving detailed fluid mechanics and geometric or wave optics. For this purpose, two appropriate techniques have been developed and applied. One is an implicit numerical method of solution; and the other is a linearized method, or fast kinetics approach, for iteration. These techniques, along with the sample results are presented in this paper.

## Governing Equations

Two-dimensional mixing layer equations are employed. The conservation equations for mass, momentum, energy, and species are written in the form

$$\frac{1}{x^\epsilon}\frac{\partial}{\partial x}(x^\epsilon \rho u) + \frac{1}{y^\sigma}\frac{\partial}{\partial y}(y^\sigma \rho v) = 0 \tag{1}$$

$$\rho u\frac{\partial u}{\partial x} + \rho v\frac{\partial u}{\partial y} = -\frac{dp}{dx} + \frac{1}{y^\sigma}\frac{\partial}{\partial y}\left(y^\sigma \mu\frac{\partial u}{\partial y}\right) \tag{2}$$

$$\rho u C_p\frac{\partial T}{\partial x} + \rho v C_p\frac{\partial T}{\partial y} = u\frac{dp}{dx} + \mu\left(\frac{\partial u}{\partial y}\right)^2 + \frac{1}{y^\sigma}\frac{\partial}{\partial y}\left(y^\sigma k\frac{\partial T}{\partial y}\right) + \rho\frac{\partial T}{\partial y}\sum_i D_i C_{pi}\frac{\partial F_i}{\partial y} - \sum_i \dot{w}_i h_i - \sum_i (h_i + \epsilon_i - h_{i+1})\frac{\alpha_i I_i}{\epsilon_i} \tag{3}$$

$$\rho u\frac{\partial F_i}{\partial x} + \rho v\frac{\partial F_i}{\partial y} = \frac{1}{y^\sigma}\frac{\partial}{\partial y}\left(y^\sigma \rho D_i\frac{\partial F_i}{\partial y}\right) + \dot{w}_i + \frac{\alpha_i I_i}{\epsilon_i} - \frac{\alpha_{i-1} I_{i-1}}{\epsilon_{i-1}} \tag{4}$$

where $x$ and $y$ denote axial and lateral distances, and $u$ and $v$ the velocities in the corresponding directions. Radial and linear flows are obtained by setting $\epsilon = 1$ and 0; and

Presented as Paper 82-0402 at the AIAA 20th Aerospace Sciences Meeting, Orlando, Fla., Jan. 11-14, 1982; submitted Jan. 25, 1982; revision received Nov. 8, 1982. 

*Member of Technical Staff. Associate Fellow AIAA.
†Member of Technical Staff.
‡Member of Technical Staff. Member AIAA.

axisymmetric and planar flows are obtained by setting $\sigma=1$ and 0, respectively. Species and mixture properties are denoted with and without subscript $i$, respectively.

The equation of state is given by

$$p=\rho RT\sum_i F_i \tag{5}$$

where $R$ is the universal gas constant. The viscosity is considered to consist of a laminar part and a turbulent part. Similar to Ref. 2, the laminar part is given by Wilke's formula and the turbulent part is based on a two-equation (turbulent kinetic energy and dissipation rate) model. The conductivity and diffusion coefficients are expressed in terms of Prandtl and Schmidt numbers.

The enthalpy and specific heat are given by

$$h=\sum_i F_i h_i \tag{6}$$

$$C_p=\sum_i F_i C_{pi} \tag{7}$$

where $h_i$ and $C_{pi}$ are tabulated functions of temperature.

For a given chemical reaction, the species production rate equation is

$$\dot{w}=k_f\Pi(\rho F_i)^{\nu_i'}-k_b\Pi(\rho F_i)^{\nu_i''} \tag{8}$$

where $k_f$ and $k_b$ are the forward and backward reaction rate constants, respectively; and $\nu_i'$ and $\nu_i''$ are the stoichiometric coefficients. The products in Eq. (8) are carried over the species participating in the reaction. The $k_f$ is a function of temperature given in Arrhenius form, and $k_b$ is expressed in terms of the equilibrium constant.

The net rate of production for any species participating in the reaction is then given by

$$\dot{w}_i=(\nu_i''-\nu_i')\,\dot{w} \tag{9}$$

For a reaction system, the total net rate of production of species $i$ is equal to the sum of the contributions for each reaction.

The molecules in each vibrational level are treated as one species. Within each vibrational level, many rotational states can be considered. However, their distributions are only represented by algebraic expressions (in Boltzmann form for equilibrium or relaxation form for rotational non-equilibrium[5]). For the lasing species, the subscript $i+1$ denotes one level higher than $i$. The radiative terms are zero except for the lasing species. At vibrational level $v$, the radiative terms are given by

$$\alpha_v I_v=\sum_J \alpha_{v,J} I_{v,J} \tag{10}$$

$$\frac{\alpha_v I_v}{\epsilon_v}=\sum_J \frac{\alpha_{v,J} I_{v,J}}{\epsilon_{v,J}} \tag{11}$$

where $J$ denotes rotational states within vibrational level $v$.

The gain is given by

$$\alpha_{v,J}=\epsilon_{v,J}\rho\,(S_{v+1,J-1}F_{v+1}-S_{v,J}F_v)\,V_{v,J} \tag{12}$$

where $\epsilon$, $S$, and $V$ are the photon energy, a line shape parameter, and the Voigt function, respectively. The representations of $S$ and $V$ are quite lengthy and are given, for example, in Refs. 1 and 2. Here, it may simply be noted that $S$ is a function of temperature only, while $V$ depends on temperature, density, and composition.

The radiation intensity is obtained from an optics solution. In contrast to Ref. 2, in which $I$ is evaluated by a laser-rate equation (limited to Fabry-Perot cavity), $I$ is evaluated in the present work by coupling to a separate geometric or wave optics code. The coupled solution by iteration is described in a later section.

It may be noted that in employing the present conservation equations, it is assumed that pressure and intensity are functions of the axial flow distance only, and that mixing is dominant only in the lateral direction. With these assumptions, the equations are in parabolic form and may be solved by a marching technique.

## Implicit Numerical Technique

The advantages of implicit methods over explicit ones are well known for fluid flow and heat transfer equations,[9] and have been analyzed and demonstrated for chemical kinetics.[10,11] These advantages pertain to numerical stability. For example, for a simple momentum transport equation, stability requires $\Delta x\le 0.5\rho u\Delta y^2/\mu$ for explicit methods. For a bimolecular forward reaction, stability for explicit methods requires $\Delta x\le u/(k_f\rho F)$. One may note that at low density, the fluid mechanical constraint is more severe; while at high density, the chemical constraint may be the dominant one. For chemical laser cavity flows, a good resolution of the flowfield generally results in a stability requirement of $\Delta x\sim 10^{-3}$ or $10^{-4}$ cm. Thus, for a cavity length of a few centimeters, many thousands of steps would be required, while several hundred steps could be sufficient for accuracy. Implicit methods, on the other hand, are free from these stability requirements.

To achieve numerical stability in both fluid mechanics and chemistry, an implicit numerical technique is formulated and employed in the present work. In accordance with the implicit method, the partial derivatives in the mixing direction, which control fluid mechanical stability, are evaluated at the forward axial location. The species source term, which controls chemical stability, is also evaluated at the forward point. In particular, the following representations are chosen in the present work

$$a\frac{\partial\phi}{\partial x}=a_K^L\frac{\phi_{K+1}^L-\phi_K^L}{\Delta x} \tag{13}$$

$$b\frac{\partial\phi}{\partial\eta}=b_K^L\left[\frac{\Delta\eta^L(\phi_{K+1}^{L+1}-\phi_{K+1}^L)}{\Delta\eta^{L+1}(\Delta\eta_T^L)}+\frac{\Delta\eta^{L+1}(\phi_{K+1}^L-\phi_{K+1}^{L-1})}{\Delta\eta^L(\Delta\eta_T^L)}\right] \tag{14}$$

$$c\frac{\partial^2\phi}{\partial\eta^2}=2c_K^L\left[\frac{\phi_{K+1}^{L+1}-\phi_{K+1}^L}{\Delta\eta^{L+1}(\Delta\eta_T^L)}-\frac{\phi_{K+1}^L-\phi_{K+1}^{L-1}}{\Delta\eta^L(\Delta\eta_T^L)}\right] \tag{15}$$

$$s_i=s_{iK}^L+\sum_j\frac{\partial s_i}{\partial F_j}\Big|_K^L(F_{jK+1}^L-F_{jK}^L) \tag{16}$$

where $\eta=y/y_m$ with $y_m$ being the centerline-to-centerline distance for a nozzle pair; subscript $K$ denotes an axial point; superscript $L$ denotes a lateral point; $\Delta x=x_{K+1}-x_K$; $\Delta\eta^L=\eta^L-\eta^{L-1}$; and $\Delta\eta_T^L=\Delta\eta^L+\Delta\eta^{L+1}$.

Equations (13-15) are used for the variables $\phi=u$, $T$, and $F_i$; and $s_i$ of Eq. (16) is the species source term which consists of the chemical production rate and the lasing transition rate terms, i.e., the last three terms in Eq. (4). One may note that the coefficients $a$, $b$, and $c$ are evaluated at the backward point. A more accurate representation is to employ an average between forward and backward points. However, this will render the equations nonlinear and iteration will be required at each step. As discussed in Ref. 9, such iterations generally are cumbersome and computation time consuming; it is usually more economical to simply reduce the step size.

The species source term is also linearized as indicated by Eq. (16). The effects of temperature and density are not included in the linearization since their changes per step are relatively small. The effect of concentration change on the Voigt function $V$ is also neglected in calculating $\partial s_i/\partial F_j$.

The conservation equations for $\phi = u$, $T$, and $F_i$ of the nonreacting species may then be arranged in the numerical form

$$A_K^L \phi_{K+1}^{L+1} + B_K^L \phi_{K+1}^L + C_K^L \phi_{K+1}^{L-1} = D_K^L \tag{17}$$

which may be solved individually for each $\phi$ by marching from $K$ to $K+1$ and using a standard tridiagonal matrix inversion procedure to obtain values at all $L$ simultaneously. The $A$, $B$, $C$, and $D$ denote coefficients known at $K$; they are different, in general, for each $\phi$.

The reaction species are coupled to each other in the form

$$A_K^L F_{i\,K+1}^{L+1} + B_K^L F_{i\,K+1}^{L} + \sum_j \frac{\partial s_i}{\partial F_j}\bigg|_K^L F_{j\,K+1}^{L} + C_K^L F_{i\,K+1}^{L-1} = D_{i\,K}^{L} \tag{18}$$

The banded system is inverted by a standard procedure to yield the coupled $F_i$'s at $K+1$ and at all $L$. In the computer program that has been developed, an option exists (in addition to the coupled system) which allows the user to consider only self-coupling (i.e., $\partial s_i/\partial F_j = 0$ except $j=i$) or noncoupling (i.e., $\partial s_i/\partial F_j = 0$ for all $j$). The self-coupling retains implicitness if the cross-coupling terms are not dominant. The noncoupling renders the species solution chemically explicit and is acceptable if all reactions are slow. These options, if applicable, facilitate the computation.

For the pressure calculation, an option exists. If flow area is prescribed, the pressure is determined by overall mass balance at each axial location. If pressure is prescribed, then the flow area is determined. The density is computed by the equation of state. The lateral velocity is calculated from the equation for conservation of mass. A similar procedure has been used previously in nonreacting nozzle flow computations.[12]

In solving the governing equations, it is assumed that the property profiles at cavity inlet are prescribed. Symmetry boundary conditions are imposed at nozzle pair centerline-to-centerline positions, i.e., at $\eta = 0$ and $\eta = 1$.

## Linearized Method for Optics Iteration

In the solution formulation process, it is observed from the conservation equations that the aerokinetics are coupled to optics only through the gain-intensity relations. Hence, the coupled equations are solved with a marching method to provide the gain distribution, which is then applied to solve the optical equations to yield the radiative intensity field. The iterative process begins by assuming a profile of intensity in solving the aerokinetics equations. Such an approach has been employed previously for a one-dimensional treatment of the laser reaction zone.[5]

In developing the present method of iteration with optics, it is observed that the radiative intensities generally have dominant effects only on the concentrations of the lasing species, and they have relatively minor effects on the fluid dynamic variables such as temperature and velocity. Therefore, once a complete or basic solution for all the aerokinetic variables is obtained, only the concentrations of the excited species need to be recalculated in subsequent iterations with optics. For these iterations, the species equations are linearized with respect to the basic solution such that the implicit chemical reaction terms evaluated and stored during the basic solution can be applied repeatedly in the subsequent iterations. To achieve higher accuracy, the complete solution is carried out again after a number of linearized solutions. If desired, several complete solutions may be taken initially before the linearized solutions are used in the iterative process.

The linearization procedure for optics iterations may be termed the "fast kinetics" approach since only the concentrations of the key species are recalculated and are solved in a rapid (linearized) manner. In this procedure, the $F_i$ and $s_i$ at any spatial point are taken as

$$F_i = F_i|_b + \Delta F_i \tag{19}$$

$$s_i = s_i|_b + \Delta s_i \tag{20}$$

where $\Delta s_i$ is given by

$$\Delta s_i = \sum_j \frac{\partial s_i}{\partial F_i}\bigg|_b \Delta F_j + \sum_j \frac{\partial s_i}{\partial I_j}\bigg|_b \Delta I_j \tag{21}$$

The values evaluated from the basic solution are denoted by the subscript $b$ and are known. The $\Delta I_j$ denotes the change from the radiative intensity applied in the basic aerokinetics solution and is known from the iterative optics solution. Therefore, substitution of Eqs. (19-21) into Eq. (4) yields a set of linearized equations for $\Delta F_i$ which may be solved simultaneously. With $\Delta F_i$, a new gain distribution is calculated algebraically, and is supplied to the optics code to obtain a new $\Delta I_j$ for the next iteration. The process is continued until the desired convergence is obtained.

The finite difference equations for the $\Delta F_i$'s have the form

$$A_{K,K+1}^L \Delta F_i|_{K+1}^{L+1} + B_{K,K+1}^L \Delta F_i|_{K+1}^{L} + \sum_j \frac{\partial s_i}{\partial F_j}\bigg|_{K,K+1}^L \Delta F_j|_{K+1}^{L}$$

$$+ C_{K,K+1}^L \Delta F_i|_{K+1}^{L-1} = D_i|_{K,K+1}^{L} \tag{22}$$

Equation (22) for $\Delta F_i$ is similar in form to Eq. (18) for $F_i$. However, the coefficients $A$, $B$, $C$, and $D$ in Eq. (22) can be averaged over $K$ and $K+1$, since they are values already known from the basic solution. The lateral partial derivatives in the species conservation equation may also be averaged over $K$ and $K+1$. The term $D_i$ in Eq. (22) contains $\Delta F_i$ at $K$ as well as $\Delta I$ at $K$ and $K+1$, which are all known in solving for $\Delta F_i$ at $K+1$. Because of the higher accuracy obtained by averaging over $K$ and $K+1$ (i.e., over $x$ and $\Delta x$), axial grid spacing coarser than that used in the basic solution may be used to reduce computation time. The number of lateral nodes may also be lowered in the iterative solution. However, the major saving in computation time with the linearization scheme is due to the fact that all reaction and radiation information are contained in the $\partial s_i/\partial F_j$ and $\partial s_i/\partial I_j$ terms, which are known from the basic solution and, therefore, need not be evaluated in the linearized solution. For a chemical system that requires hundreds of reactions and many species, there exists a several-fold reduction in computation time compared to the complete or basic solution.

It may be noted that the number of species that are considered to undergo concentration change due to changes in radiative intensity may be limited to only a few of the lasing species, or it may include other reacting but nonlasing species. The number of species that need to be considered in the iteration depends on the particular system, and is an input to the computer program.

In the computer program that has been developed, chemical reactions and species are input by the user. Hence, various chemical systems may be investigated without internal changes to the program. The program employs dynamic dimensioning, namelist input, and modular design. It contains minimal data array relocation, minimal table function search, and debug print option.

## Results and Discussion

Using the advanced cavity code (ACC) computer program developed a sample case of an HF laser is chosen to illustrate the numerical results. The oxidizer stream consists of F, $F_2$, DF, $N_2$, and He. The fuel stream, injected from a much smaller nozzle, consists of only $H_2$. For the lasing species HF, seven vibrational levels (including ground state) are considered. Each of the seven vibrational levels represents a chemical species, and each is considered to consist of 16 rotational states. Additional species generated by chemical reactions are H, two additional levels of $H_2$, and an additional level of DF and of $N_2$. Thus, a total of 18 species are considered in the system. The number of chemical reactions treated is 143. The temperature and velocity profiles at cavity inlet are indicated in Fig. 1. Sixteen lateral grid points are used, and the grid spacing is also shown in Fig. 1. Smaller grid spacing is taken in the regions of steeper property gradients. The fuel stream, being very small, is considered to have uniform properties initially and is represented by only four grid points.

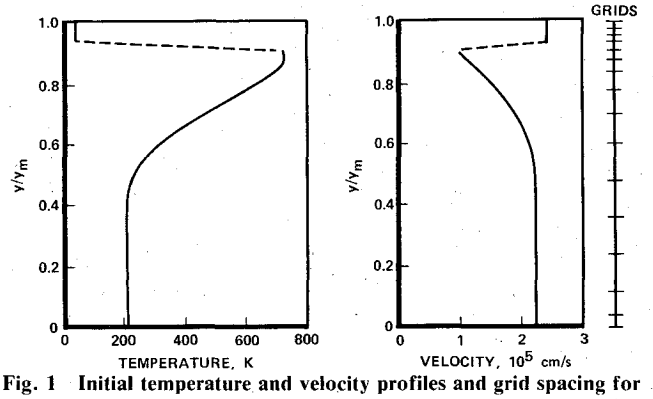


Fig. 1 Initial temperature and velocity profiles and grid spacing for sample problem.

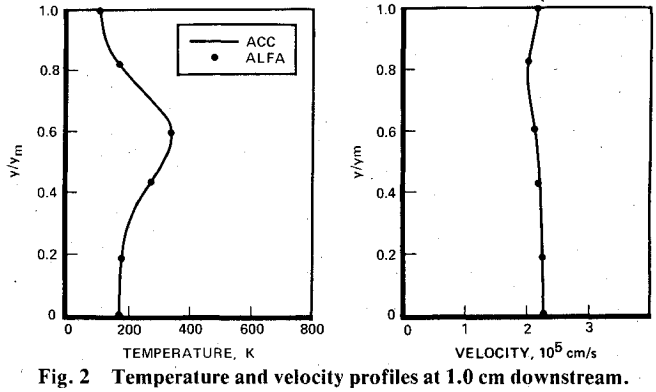


Fig. 2 Temperature and velocity profiles at 1.0 cm downstream.

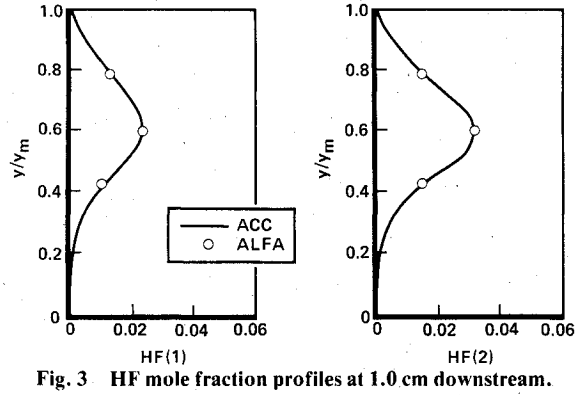


Fig. 3 HF mole fraction profiles at 1.0 cm downstream.

To verify the numerical accuracy of the computational method and to compare the machine computation time, the same case is also calculated using the industrial reference computer program ALFA.[2] Identical initial conditions, lateral grid spacing, and chemical data are used in both the present program and ALFA.

The results are illustrated in Figs. 2-7. In these figures, the continuous curves are results based on the present program while the points indicate results from ALFA. Figure 2 shows the temperature and velocity profiles at 1.0 cm downstream, and Fig. 3 shows the concentrations of HF(1) and HF(2) at the same axial location. Figures 4-6 show the distributions of pressure, centerline temperatures, and some centerline concentrations, respectively. The distance $x$ is measured from cavity inlet. The small signal gain, averaged over $y_m$, for several transitions is shown in Fig. 7. These figures indicate excellent agreement between the present and ALFA results.

The execution time, for this particular sample run, on the CDC CYBER 176 machine is 24 s for the present program and 708 s for ALFA. If more lateral nodes are used, the com-

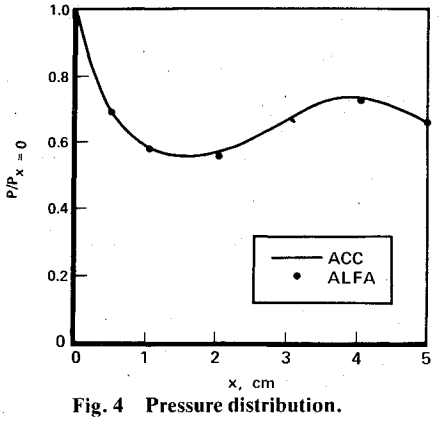


Fig. 4 Pressure distribution.

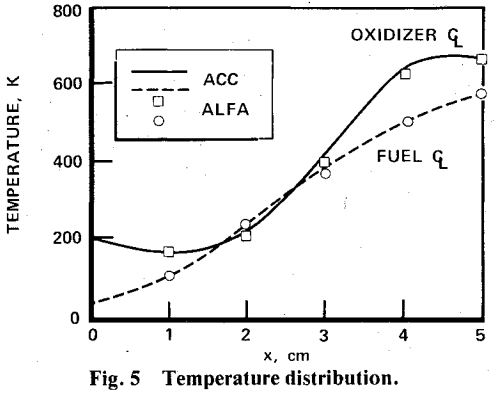


Fig. 5 Temperature distribution.

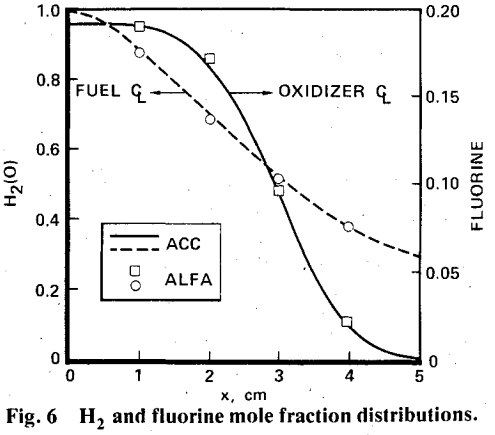


Fig. 6 $H_2$ and fluorine mole fraction distributions.

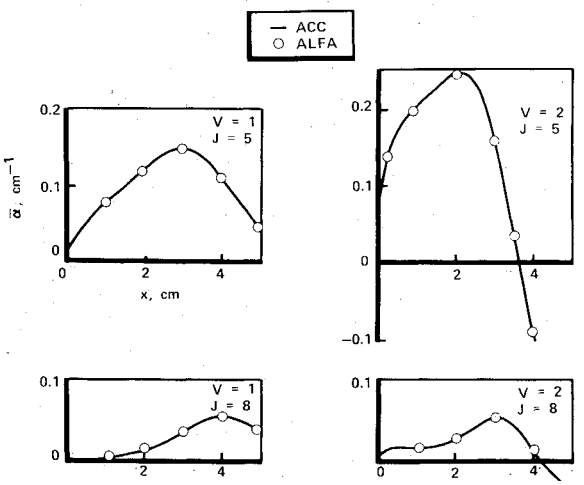


Fig. 7 Small signal gain distributions.

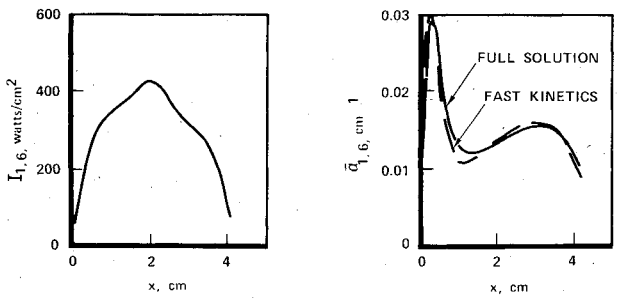


Fig. 8 Comparison of linearized (fast kinetics) solutions to full solution.

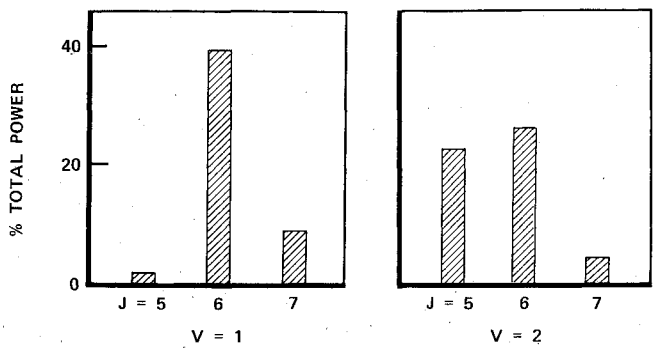


Fig. 9 Power spectral content with rooftop resonator.

parison in computation time is even more favorable for the present program since the fluid-mechanical step-size stability for the explicit numerical method used in ALFA requires $\Delta x \sim \Delta y^2$. However, sample results obtained using 31 nodes indicate that the values obtained with 16 nodes are sufficiently accurate, as the results generally differ by only a couple of percent. It may be pointed out that ALFA contains a node-cutting scheme which, if exercised, will reduce its computation time to less than 2 min. It may also be noted that ALFA contains some options, such as lateral pressure gradient in supersonic regions and oblique shock in base section, which have not been treated in the present program.

For the sample case of HF system, the stability (for explicit methods) appears to be controlled by fluid mechanics rather than chemistry. For chemical systems involving very rapid rates, the reduction in computation time using implicit methods is even more drastic as demonstrated in Refs. 10 and 11.

To illustrate the optics coupling and the linearized iteration method, a rooftop resonator code is chosen for simplicity. During iteration, an algebraic rotational nonequilibrium model is used. The rooftop simulation and the rotational nonequilibrium model have been discussed in Ref. 5.

Figure 8 illustrates the accuracy of the linearized (fast kinetic) solution. The radiation intensity obtained from optics after three iterations is shown on the left of the figure. With this intensity field, the gain for the next iteration is computed from the present program using both the complete solution and the linearized solution for comparison. It is seen that the linearized method yields sufficiently accurate results. As the iteration process approaches convergence, the difference between the full solution and the linearized solution further diminishes. For the sample linearized solution, the execution time on a CDC machine is about 7 s per iteration. The power spectral content obtained with the rooftop resonator, after 40 iterations and reaching convergence, is illustrated in Fig. 9.

Comparisons of intensity and power with ALFA results have not been made; since ALFA is restricted to plane parallel mirrors without downstream radiation feedback, whereas the present results are for realistic optics with upstream-downstream radiative interaction.

In general, tens or hundreds of aerokinetics-optics iterations are required to achieve convergence. Numerical methods based on explicit methods and without some approximation procedure (linearization) will require prohibitively long machine computation time. On the other hand, with the present implicit method and the linearized iterative procedure, a converged solution using real optics and detailed fluid mechanics can be obtained in about 10 min of CDC time.

In correlating analysis with experimental data, the ALFA (or LAMP) program has been widely used.[6-8] Since the present program yields practically identical results as ALFA, the correlations observed previously are expected to prevail for the present program also.

## Conclusions

Based on the present investigation, the following conclusions may be reached.

1) The accuracy of the present two-dimensional aerokinetics computation procedure has been verified by comparison with the industry reference program ALFA.

2) Application of the implicit numerical integration technique and the fast kinetics numerical concept has improved execution time significantly.

3) The feasibility of two-dimensional flow analysis and geometric/wave optics coupling has been demonstrated.

## Acknowledgments

The authors wish to thank Dr. J. J. Vieceli and Dr. L. F. Moon for their discussions, interests, and assistance during the course of the present investigation.

## References

[1] Hendricks, W. L., Thoenes, J., McDanal, A. J., Mikatarian, R. R., and Martin, W. D., "Laser and Mixing Program (LAMP) Theory and User's Guide," Lockheed Missiles and Space Co., Rept. RH-CR-77-4, Aug. 1976.

[2] Thoenes, J., Hendricks, W. L., Kurzius, S. C., and Wang, F. C., "Advanced Laser Flow Analysis (ALFA) Theory and User's Guide," Lockheed Missiles and Space Co., Rept. AFWL-TR-78-19, Feb. 1979.

[3] King, W. S. and Mirel, H., "Numerical Study of a Diffusion-Type Chemical Laser," *AIAA Journal*, Vol. 10, Dec. 1972, pp. 1647-1654.

[4] Tripodi, R., Coulter, L. J., Bronfin, B. R., and Cohen, L. S., "Coupled Two-Dimensional Computer Analysis of CW Chemical Mixing Lasers," *AIAA Journal*, Vol. 13, June 1975, pp. 776-784.

[5]Yang, T. T., "Modeling of CW HF Chemical Lasers with Rotational Non-Equilibrium," *Journal de Physique,* Vol. C9, Nov. 1980, pp. 51-57.

[6]Mikatarian, R. R. and McDanal, A. J., "Analytical and Experimental Correlation of the HF Chemical Laser Flow Data," AIAA Paper 75-39, Pasadena, Calif., Jan. 1975.

[7]Hendricks, W. L., Kurzius, S. D., and Mikatarian, R. R., "Comparisons Between LAMP Theoretical Predictions and Experimental Spectroscopic and Chemical Laser Performance," AIAA Paper 77-656, Albuquerque, N. Mex., June 1977.

[8]O'Keefe, D., Sugimura, T., Behrens, W., Bullock, D., and Dee, D., "Comparison of LAMP and BLAZER Code Calculations with TRW CL XV Measurements," *Optical Engineering,* Vol. 18, July-Aug. 1979, pp. 363-369.

[9]Hornbeck, R. W., "Numerical Marching Techniques for Fluid Flows with Heat Transfer," NASA SP-297, 1973.

[10]Tyson, T. J. and Kliegel, J. R., "An Implicit Integration Procedure for Chemical Kinetics," AIAA Paper 68-180, New York, N. Y., Jan. 1968.

[11]Quan, V., Melde, J. E., Kliegel, J. R., Nickerson, G. R., and Frey, H. M., "Kinetics Performance of Barrier-Cooled Rocket Nozzles," *Journal of Spacecraft and Rockets,* Vol. 5, Oct. 1968, pp. 1136-1142.

[12]Rae, W. J., "Some Numerical Results on Viscous Low-Density Nozzle Flows in the Slender-Channel Approximation," *AIAA Journal,* Vol. 9, May 1971, pp. 811-820.